Colloid Polym Sci (2004) 282: 495–501
DOI 10.1007/s00396-003-0973-3

B. Granqvist
A. Helminen
M. Vehviläinen
V. Ääritalo
J. Seppälä
M. Lindén

Biodegradable and bioactive hybrid organic–inorganic PEG-siloxane fibers. Preparation and characterization

Received: 1 April 2003
Accepted: 23 June 2003

B. Granqvist · M. Lindén (✉)
Department of Physical Chemistry,
Åbo Akademi University, Porthansgatan
3–5, 20500 Turku, Finland
E-mail: mika.linden@abo.fi

A. Helminen · J. Seppälä
Department of Chemical Technology,
Laboratory of Polymer Technology,
Helsinki University of Technology,
P.O. Box 6100, 02015 Hut, Finland

M. Vehviläinen
Institute of Fiber Materials Science,
Tampere University of Technology,
P.O. Box 589, 33101 Tampere, Finland

V. Ääritalo
Biomaterials Research, Institute of
Dentistry, University of Turku,
Lemminkäisenkatu 2,
20520 Turku, Finland

Abstract A mixture of triethoxysilanefunctionalized poly(ethylene glycol), f-PEG, and tetraethoxysilane, TEOS, was used as precursors in the preparation of continuous hybrid f-PEG-siloxane sol–gel derived fibers. The fibers were spun by extrusion through a spinneret. The thus prepared fibers had a diameter of 20–50 μm. ^{29}Si-CPMAS NMR measurements confirmed that the functionalized PEG is incorporated into the siloxane network through covalent bonds. The hybrid fiber elasticity was much higher than that of fibers spun from sols with TEOS as the only source for silica. However, the f-PEG chain length plays a crucial role for the spinnability of the sol, since, as a result of bridging flocculation, macroscopic phase separation occurred readily with increasing chain length of the f-PEG. The fibers were shown to be effective substrates for the nucleation and growth of bone-like hydroxyapatite.

Keywords Silica · Fiber · Hybrid · Bioactive · Biodegradable

Introduction

The use of bioactive, ceramic materials has proven to be a cost-effective and efficient means of replacing or healing tissues in the body. The nucleation and growth of calcium phosphate on the implant surfaces is considered to be crucial for a strong adhesion between the implant and the surrounding tissues [1, 2]. Such materials can be prepared by conventional glass processing or by low-temperature sol–gel techniques. Although most materials are available as powders and granules, macroscopic morphology control is in many cases desirable and allows for an easier processing and handling of the materials. The sol–gel technique is a very flexible means for morphology control, and films, fibers, and monolithic structures can be prepared with the right choice of synthesis composition and conditions [3]. For example, the bioactivity and biocompatibility of titanium metal, a frequently used load-bearing implant, can be dramatically improved by coating the surface with a bioactive thin film of silica or titania [4]. Recently, biodegradable [5, 6]' and bioactive silica-based fibers [7, 8, 9] have been prepared, which readily can be further processed to mats or other structures. Furthermore, because of the low-temperature synthesis conditions, drugs can be directly incorporated into the fiber matrix and the diffusion controlled drug release properties of sol–gel derived silica fibers have been demonstrated [9]. In vitro bioac-

Scheme 1 Functionalization of PEG with (3-isocyanatopropyl) triethoxysilane

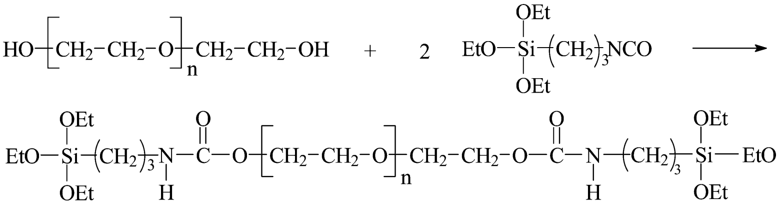

tivity, i.e., the nucleation and growth of carbonated hydroxy apatite on the materials surface when exposed to a simulated body fluid, has been demonstrated both for silica [9] and $CaO–SiO_2–P_2O_5$ [7, 8] fibers. Depending on the calcium and phosphorous content, the latter maintain their bioactivity even after thermal stabilization at temperatures up to 700 °C, although some hydroxy apatite seemed to have crystallized in the heat-treated fibers already prior to exposure to the simulated body fluid (SBF). However, the fully inorganic nature of these fibers, regardless of their silica content, has some disadvantages because of their inherent low elasticity. One means of enhancing the elastic properties is to prepare hybrid organic–inorganic materials composed of nanocomposite networks, where the organic portion provides certain flexibility to the network while the inorganic portion maintains the mechanical properties at a desired level. Such hybrid materials can be classified according to the interlinking between the two types of networks. In class I materials the organic molecules are embedded within the inorganic matrix, while strong covalent linkage is formed between the inorganic and the organic phases in class II materials [10]. These hybrid materials can also be highly biocompatible and biodegradable, if the organic network is biocompatible, as demonstrated for class II poly(ε-caprolactone)–silica hybrid materials by Tian et al. [11, 12, 13, 14, 15]. However, these materials were not obtained in the form of fibers. The purpose of the present study was to take advantage of the enhanced mechanical and elastic properties of hybrid nanocomposites in the preparation of biodegradable and bioactive silica-based, class II sol–gel derived fibers. We chose poly(ethylene glycol), PEG, as the organic network former, since it is completely soluble in both water and ethanol and it is also known to be biocompatible. The fibers were characterized by ^{29}Si-NMR, SEM, mechanical, and in vitro tests, respectively.

Experimental

Synthesis of triethoxysilicon end-capped poly(ethylene glycols)

Poly(ethylene glycols) (PEG) were bought from Fluka Chemie GmbH, Buchs, Switzerland. Four different PEGs were used and they differed in their nominal molecular weights: 1,000, 6,000, 20,000 and 35,000 g·mol^{-1} (denoted as $PEG_{1,000}$, etc). (3-Isocyanatopropyl)triethoxysilane (IPTS) from ABCR GmbH, Karlsruhe, Germany, was used in the functionalization step.

Linear PEGs were terminated with (3-isocyanatopropyl)triethoxysilane (Scheme 1). First the polymers were dissolved in hot toluene (1:3 w/v) in a glass vessel and about 1/10 of the solvent was distilled in order to remove the water adsorbed to the hydrophilic PEG. Then IPTS was added to the mixture in a nitrogen atmosphere and it was refluxed for 30 min at 120°C. The amount of IPTS was calculated from the hydroxyl value of the PEG given by the supplier. Excess of stoichiometric amount of IPTS was used as shown in Table 1. The mixture was allowed to cool and after crystallization the functionalized PEG (f-PEG) was filtered and washed with toluene. The low melting point prevented the filtering of the crystallized f-$PEG_{1,000}$. Thus, the solvent and unreacted IPTS were removed by distillation under vacuum at 140°C. Finally the products were dried under vacuum at room temperature for 72 h.

Average molecular weights ($\bar{M}_n$ and $\bar{M}_w$) and molecular weight distributions (MWD) were determined relative to polystyrene standards by size exclusion chromatography (SEC). The Waters Associates (Milford Mass., USA) system was equipped with a Waters 700 satellite wisp injector, a Waters 510 HPLC solvent pump, four linear PL gel columns (10^4, 10^5, 10^3, and 100 Å) connected in series, and a Waters 410 differential refractometer. All samples were analyzed at room temperature. Chloroform from Riedel-de Haën Ag, Seelze, Germany (stabilized with 1% ethanol) was used as eluent and was delivered at a flow rate of 1.0 ml·min^{-1}. The samples were dissolved in chloroform at a concentration of 0.1% (w/v). The injection volume was 200 μl.

For ^{13}C NMR measurements, the samples were dissolved in chloroform-d$_1$ (Fluka, deuteration not less than 99.8%) in 10-mm NMR tubes at room temperature. The sample concentration was 10% by weight. NMR spectra were recorded on a Varian Gemini 2000 (Palo Alto, Calif., USA) 300 MHz spectrometer working at 75.445 MHz for carbon.

Table 1 Properties of PEGs before and after the functionalization

Name (-nominal M):	Hydroxyl value[a] ((mgKOH) g^{-1})	M(PEG)[b] (g mol^{-1})	NCO:OH ratio	OH conversion (%)
PEG-1000	116.2	970	1.05	100
PEG-6000	18.9	5,940	2.0	57
PEG-20000	5.2	21,600	2.0	28
PEG-35000	3.6	31,600	2.0	42

[a] Given by Fluka Chemie GmbH, Buchs, Switzerland.
[b] Calculated from hydroxyl value.

Sol preparation and fiber spinning

Sols were prepared by dissolving 0.5 or 1.0 wt% with regards to the total amount of SiO_2 of f-$PEG_{6,000}$ or 4 or 20 wt% of f-$PEG_{1,000}$ into 110 g of ethanol (99.5%). Tetraethyl orthosilicate $Si(OC_2H_5)_4$ (TEOS) (500 g) was then added and the mixture was placed into an ice bath. Ultra purified distilled water and HNO_3, (65%), was added under vigorous stirring to give an *r* value ($r=[H_2O]/[TEOS]$) of 2. The clear sol was poured into an evaporation bowl and kept at 40 °C for 21–24 h depending on the rate of hydrolysis and polycondensation reactions. These reactions were followed by measuring the amount of distilled ethanol per unit time by Sartorius BP 2100 S scales(Göttingen, Germany), which was connected to a PC running the Weightwin program (free software of A&D Co. Ltd., Tokyo, Japan). Evaporation was stopped when the amount of evaporated ethanol was decreased to 0.1–0.2 g/min. Thereafter the sol was cooled to RT and the reaction rate was followed by viscosimetry (DV II+, Brookfield Engineering Laboratories Inc., Middleboro, Mass., USA) with a spindle speed of 0.3 rpm (LV2 disc shaped spindle).

Fibers were spun by dry spinning using the air gap of 4 m before collection. The general features of the setup have been described in detail previously [16]. The spinnerets were made of a gold/platinum mixture (Wetzel Gröbzig Micro Products, Grenzach-Wyhlen, Germany, Ø = 65 μm, with the number of holes being either 3, 6, or 10). The fibers were collected either on a 3.7-m long circular wire or around a piece of rotating cardboard.

Fiber spinning was started when the viscosity of the sol reached 5,500–8,000 cP and continued until the gel point was reached or until all of the sol was consumed. The as-spun fibers were dried for 2 h at 50 °C, if not otherwise mentioned, and stored in a sealed sachet of aluminium foil.

Alternatively, fibers were drawn directly from the sol using the glass rod method. The sols had the same composition as those used for spinning. However, no external cooling was used during the hydrolysis of the TEOS. The sol was first kept at 40 °C and then cooled to RT before the sol fiber drawing. The fibers thus prepared were air dried at RT, without any subsequent heat treatment.

Fiber characterization

Mechanical testing

Titer, tenacity and elongation of the fibers were determined using Vibroskop and Vibrodyn equipment (Lenzing AG, Lenzing, Austria), respectively. The tensile test was performed with a constant rate of elongation according to DIN 51221 and 53816. The rate of elongation was 2 mm/min and gauge length 20 mm. Tenacity is indicated in cN/tex, elongation in percent, related to the gauge length and titer in dtex. Tenacity of the fibers were converted to MPa units using the following equation:

$$\text{Tenacity}[\text{MPa}] = \text{Tenacity}[\text{N/tex}] \times 1000 \times \text{density}\left[\text{g/cm}^3\right]$$

where 1.6 g/cm^3 was used as the value for the fiber density.

^{29}Si NMR measurements were carried out using a Chemagnetics Inc. (Fort Collins, Colo., USA) CMX infinity spectrometer operating at 270 MHz at Fortum Oil and Gas Oy Technology Centre in Porvoo, Finland. A probe with 10 mm zirconia rotors was used. Cross-polarization spectra were acquired using a 5 ms contact time, 5 s recycle delay, 30 kHz fields, MAS speed about 3.5 kHz, and transients between 5,000 and 15,000. The ^{29}Si MAS spectra were acquired using 45° excitation pulse, 300 s recycle delay, MAS speed about 3.5 kHz, and transients between 188 and 400. The MAS experiments were run without 1H decoupling.

Scanning electron microscopy (SEM) images were recorded on a S360 from LEO Electron Microscopy Ltd., Cambridge, UK.

Fiber dissolution and in vitro tests

The in vitro bioactivity of the samples was tested using a simulated body fluid, SBF [17], solution prepared by dissolving the reagent chemicals NaCl, $NaHCO_3$, KCl, $K_2HPO_4 \cdot 3H_2O$, $MgCl_2 \cdot 6H_2O$, $CaCl_2 \cdot 2H_2O$, and Na_2SO_4 into deionized water. The SBF was buffered at physiological pH 7.40 with tris(hydroxymethyl)aminomethane and hydrochloric acid. The samples were placed in a shaking water bath (Heto-Holten A/S, Allerod, Denmark, SBD 50, 160 strokes per minute with stroke amplitude 36 mm) having a constant temperature of 37 °C.

The sample solutions were monitored for calcium, phosphate and silica concentrations as a function of immersion time. The calcium concentrations were determined with an atomic absorption spectrophotometer (AAS, Perkin-Elmer 460—Perkin-Elmer Life and Analytical Sciences, Inc., Boston, Mass., USA). The phosphate and silica concentrations were determined by the molybdenum blue method by UV-Vis spectroscopy (Hitachi Europe Ltd., Maidenhead, UK, Model 100–60).

Results and discussion

f-PEG characterization

The extent of the functionalization was evaluated with ^{13}C NMR. Overlapping signals prevented the use of more sensitive ^{1}H NMR in structure evaluation. As shown in Table 1 the hydroxyl group conversion was 100% for $PEG_{1,000}$. Resonances at 72.5 and 61.5 ppm disappeared with functionalization and new peaks appeared at 156.2 ppm caused by the urethane bond, at 69.5 and 63.6 ppm caused by the PEG unit next to urethane bond, at 43.3, 23.2, and 7.5 ppm caused by the propyl chain in reacted IPTS, and 58.2 and 18.2 ppm caused by the ethoxy groups (see Fig. 1). The degree of–OH conversion decreased with increasing PEG molecular weight, as previously observed for the functionalization of poly-lactides by IPTS [18].

Importantly, no free isocyanates were detected at 122.2 ppm, indicating that unreacted IPTS was removed from the f-PEGs produced. The results in Table 1 show that the OH conversion decreased with increasing molecular weight of the PEGs even though higher excess of IPTS was used with longer PEG. Thus the f-PEGs with higher molecular weight were not as highly functionalized as f-PEG$_{1,000}$. Theoretically, a successful functionalization should increase the molecular weight of the PEGs by 490 g·mol^{-1}. A slight increase in molecular weights was detected by SEC, which confirmed the functionalization and more importantly ruled out premature polymerization of the triethoxysilane functionalized PEG's.

Dependence of fiber spinnability on sol pH and f-PEG molecular weight

The optimum pH for fiber drawing was determined for f-PEG$_{1,000}$/TEOS sols with an f-PEG/TEOS wt% ratio of 5.76%, which corresponded to 20 wt% f-PEG$_{1,000}$/SiO$_2$, at an *r* value of 2. The pH of the sols was varied between 0.5 and 3 through addition of HNO$_3$, and their suitability for fiber spinning was studied by the glass rod method. Fibers were obtained for in the pH range 0.5–1, while the spinnability was poor for sols with pH between 1.5 and 3. However, since the pH = 1, sol remained spinnable for a longer time and it was chosen for further studies. This pH is the same as that found being optimal for fiber spinning from TEOS based sols [6], and suggests that the pH dependence of the hydrolysis–condensation reactions of the mixed f-PEG$_{1,000}$/TEOS systems are very similar. It has previously been shown that the polymerization of both silicon alkoxide [3] and class II siloxane-poly (propyleneoxide) gels [19] follows the reaction-limited cluster–cluster aggregation mechanism, RLCCA, under acidic conditions, if the poly(propyleneoxide) chain is short. This leads to the formation of nearly linear chains with few branches, structures that are ideal for fiber spinning. In the case of siloxane-poly(propyleneoxide) gels, a change from RLCCA to diffusion limited monomer–cluster aggregation is observed with increasing PPO chain length [19], which lead to a branching of the aggregates. We also observed a decrease in the spinnability of f-PEG$_{6,000}$/TEOS and f-PEG$_{35,000}$/TEOS sols, respectively, with increasing f-PEG/TEOS ratio. This effect could originate from the formation of branched aggregates. However, the lower degree of functionalization of these f-PEG precursors could also contribute to the poorer spinnability of these sols, since it is known that bridging flocculation, which leads to phase separation, readily occurs in PEG/TEOS sols with long PEG chain lengths. Therefore, the f-PEG$_{1,000}$ was chosen for pilot scale fiber spinning tests. The sols remained spinnable in the f-PEG$_{1,000}$/TEOS range 0.58–5.76%.

Fiber characterization

SEM

A representative SEM image of hybrid f-PEG$_{1,000}$/TEOS (5.76%) machine-spun fibers is shown in Fig. 2. The fibers are 8-shaped with diameters in the range of 25–50 μm. The textural features are similar to that observed for fibers spun from sols where TEOS was the only source for silica [9].

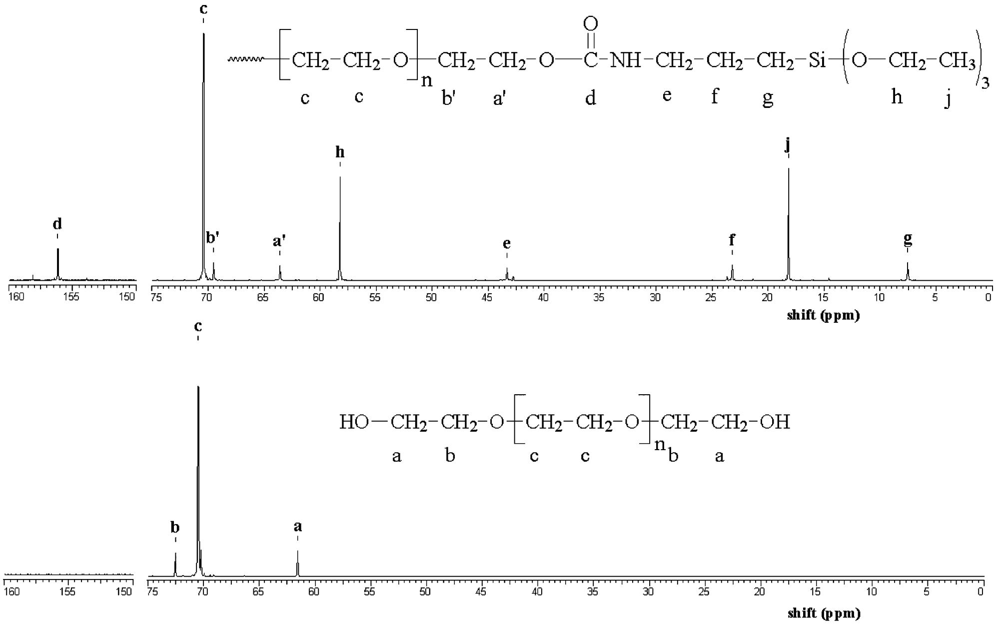

Fig. 1 ^{13}C NMR spectra recorded for PEG$_{1,000}$ (lower) and f-PEG$_{1,000}$ (upper spectrum). See *inset* for resonance frequency indexing

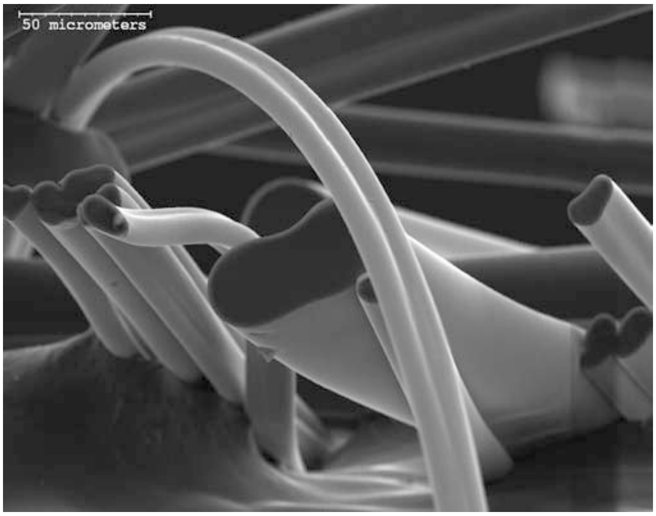

Fig. 2 SEM image of machine-spun heat-treated hybrid f-PEG$_{1,000}$/TEOS (5.76%) fibers

The high flexibility of the fibers is clearly seen in the SEM image. Both individual and bundled fibers were observed in all cases. Fibers prepared by the glass rod technique showed the same general shape as the machine-spun fibers, but their diameters were in the range of 75–150 μm.

^{29}Si-NMR

The degrees of condensation of the f-PEG and the TEOS, respectively, were determined by CP MAS and MAS ^{29}Si-NMR for hand-made and machine-spun f-PEG$_{1,000}$/TEOS 5.76% fibers. The silane groups in the f-PEG give peaks in the region -50 to -70 ppm, while those originating from TEOS show resonance in the -85 to -120 ppm region. Therefore, they can be easily separated from each other. For the f-PEG, only T^2 peaks at -57 ppm and T^3 peaks at -64 ppm were detected, with a T^3/T^2 ratio of 3.2 for machine-spun and 5.6 for hand-made fibers, respectively, as measured by CP MAS. Although cross-polarization measurements do not strictly give a quantitative measure for the degree of condensation, at least semi-quantitative data can be obtained [20]. Even if the absolute number may be slightly off the correct one, it is safe to assume that the f-PEG has been incorporated into the siloxane network with a high degree of condensation. Fully quantitative MAS measurements were performed in order to determine the degree of condensation of the inorganic siloxane network resulting from the hydrolysis and condensation of TEOS. The measured Q^n values are summarized in Table 2.

Comparing the T^3/T^2 ratios to the Q^4/Q^3 ratios, it can be seen that the degree of condensation of the Q units is lower than that of the T units, which further stresses the high degree of condensation of the f-PEG. Furthermore, the degree of condensation of the machine-spun f-PEG$_{1,000}$/TEOS 5.76% fiber is lower than that of the other two studied fibers, in agreement with the CP MAS results obtained for the T units. It has been shown that a clear increase in the degree of condensation of silica fibers is observed if the fibers, as in our case, are spun and dried in air, as compared to fibers spun and/or dried under inert atmosphere [21]. It is clear that the processing step has a pronounced influence on the degree of condensation, as also seen in the differences observed between hand-made and machine-spun f-PEG$_{1,000}$/TEOS fibers. This could be due to a kinetic effect, since it has been shown that the presence of hydration water originating from hydrophilic solubilizates, may lead to an increase of the degree of silicate condensation [9]. The presence of the hydrophilic PEG chains in the fibers can therefore allow for an increase in the degree of silicate condensation with time. Therefore it is clear that the measured T and Q values should not be taken as any measure of the silicate distributions in the sols, which has been shown to be dramatically lower in spinnable sols [22].

Mechanical properties

The tenacity and elongation values determined for different f-PEG/TEOS fibers are given in Table 3, and compared with corresponding values obtained for f-PEG/TEOS 0%. The influence of drying conditions was also investigated. It is clearly seen that drying of the fibers at temperatures above RT has a detrimental effect on the mechanical properties, in agreement with previous studies [21].

The f-PEG$_{6,000}$ fibers are very strong, but possess a low elasticity. However, with the f-PEG$_{1,000}$ both strong and very elastic fibers can be obtained. No direct correlation between the sol viscosity at the time of fiber spinning and the mechanical properties of the fibers could be found, since the standard deviation in the

Table 2 Distribution of the silicate units in the matrix as determined by ^{29}Si MAS NMR

	Q^2	Q^3	Q^4	Q^4/Q^3
Hand made f-PEG$_{1000}$/TEOS 5.76% (no heat treatment)	6.1%	53%	40.9%	0.77
Machine spun f-PEG$_{1000}$/TEOS 5.76% (heat treated)	11.1%	62.2%	26.6%	0.42
Machine spun f-PEG$_{1000}$/TEOS 0% (no heat treatment)	8.7%	54.6%	*36.7%*	0.67

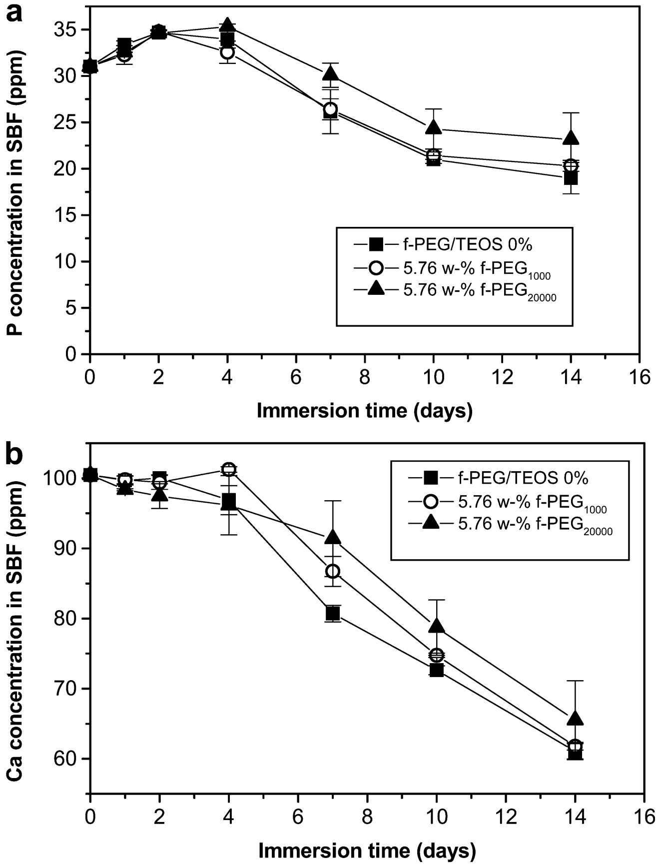

Fig. 3 **a** The change of P concentration in SBF as a function of time, for two hand-made fibers, f-PEG$_{1,000}$/TEOS (5.76 wt%) and f-PEG$_{20,000}$/TEOS (5.76 wt%), and one machine-spun fiber f-PEG/TEOS (0 wt%). **b** The change of Ca concentration in SBF as a function of time, for two hand-made fibers, f-PEG$_{1,000}$/TEOS (5.76 wt%) and f-PEG$_{20,000}$/TEOS (5.76 wt%), and one machine-spun fiber f-PEG/TEOS (0 wt%)

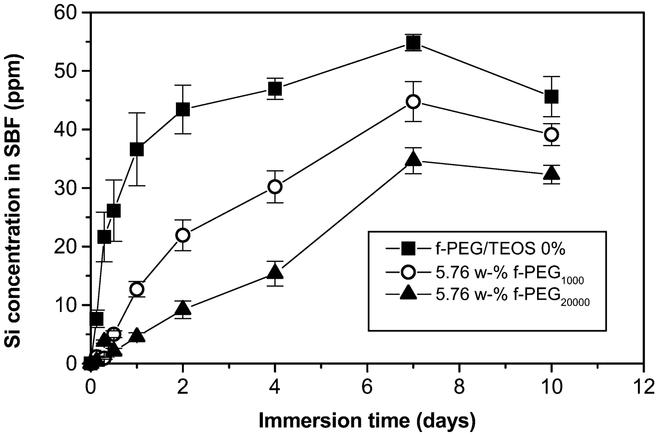

Fig. 4 The dissolution as a function of time, for two hand-made fibers, f-PEG$_{1,000}$/TEOS (5.76 wt%) and f-PEG$_{20,000}$/TEOS (5.76 wt%), and one machine-spun fiber f-PEG/TEOS (0 wt%)

measurements was quite high. This can be contributed to the fact that the variation in fiber diameter was also quite large. However, machine-spun f-PEG$_{1,000}$/TEOS 5.76% fibers, which were allowed to dry in air at RT for a week, possessed clearly higher tension values and much higher elongation values than those measured for the heat-treated (50°C/2 h) fibers. The tension values of the hybrid fiber were about 100% and the elongation value 600–1,000% higher than those measured for the fully inorganic fiber (f-PEG 0%). There is no doubt that the hybrid fibers dried at RT are superior to the other fibers in combining both a high strength and a high degree of elasticity.

In vitro analysis

The ability of hybrid f-PEG$_{1,000}$/TEOS 5.76% and f-PEG$_{20,000}$/TEOS 5.76% fibers to serve as substrates for the nucleation and growth of carbonated hydroxyapatite was studied in vitro by keeping some of the fibers in a simulated body fluid and monitoring the change in calcium and phosphate concentration with time. A f-PEG/TEOS 0% fiber, which was shown to be bioactive [6], was used as a reference. The results are summarized in Fig. 3a and b, respectively. A pronounced decrease in both the calcium and phosphate concentrations is observed after 4 days of immersion for all fibers studied.

Table 3 Tenacity and elongation values for different f-PEG/TEOS fibers

Sol	Drying	Tenacity		Elongation	Std-dev of elongation	Number of tests
		(cN/tex)	(MPa)	(%)	(%)	
0 wt% f-PEG	Dried at 50°C	27–32	440–500	1.5–3	42	41
4 wt% f-PEG$_{1000}$	Dried at 50°C	18–28	300–450	4–8	26	18
1 wt% f-PEG$_{6000}$	Dried at 50°C	35–40	600	7	21	40
0.5 wt% f-PEG$_{6000}$	Dried at 50°C	60–100	1,000–1,600	1–5	30	34
20 wt% f-PEG$_{1000}$	Dried at 50°C	7–13	140–200	4–8	40	86
20 wt% f-PEG$_{1000}$	Dried at RT without subsequent heat treatment	65	1,050	18	32	10

These ions were consumed from the media and this is indirect evidence of the calcium phosphate formation. The calcium phosphate will then be transformed into hydroxyapatite by dissolution–reprecipitation [23, 24]. Therefore, one can conclude that both hybrid fibers are bioactive and that their bioactivities are on the same level as that of the reference fiber.

However, the silica dissolution rate of the fibers was quite different, as shown in Fig. 4. The dissolution rates represent the degradation of the fibers, and were clearly lower than that of the reference fibers, which are connected to the higher degree of condensation and the higher diameters measured for the hand-made hybrid fibers. However, all fibers degrade in SBF, which make them suitable for biological applications.

Conclusions

Hybrid (class II) biocompatible, biodegradable and bioactive class II hybrid PEG-siloxane fibers have successfully been prepared. The mechanical properties of the hybrid fibers are superior to corresponding pure siliceous fibers, and both the strength and the flexibility of the fibers can be increased at the same time, without loosing any of the bioactive response. The fibers should be especially suitable for reinforcement of biopolymers.

Acknowledgements The Finnish National Technology Agency, TEKES, is gratefully acknowledged for financial support. Dr. Andrew Root, Fortum Gas and Oil Oy, Porvoo, Finland, is acknowledged for the ^{29}Si-MAS NMR measurements.

References

1. Martin RI, Brown PW (1994) J Mater Sci: Mater Med 5:96
2. Serro AP, Fernandes AC, Saramago B, Lima J, Barbosa MA (1997) Biomaterials 18:963
3. Brinker J, Scherer GW (1990) Sol–gel science. Academic Press, San Diego
4. Li P, Ohutski C, Kokubo T, Nakanishi K, Soga N, de Groot K (1994) J Am Ceram Soc 77:1307
5. Kursawe M, Glaubitt W, Therauf A (1998) J Sol-Gel Sci Technol 13:267
6. Peltola T, Jokinen M, Veittola S, Rahiala H, Yli-Urpo A (2001) Biomaterials 22:589
7. Oréfice RL, Hench LL, Clark AE, Brennan AB (2001) J Biomed Mater Res 55:460
8. Domingues RZ, Clark AE, Brennan AB (2001)J Biomed Mater Res 55:468
9. Czuryszkiewicz T, Ahvenlammi J, Kortesuo P, Ahola M, Kleitz F, Jokinen M, Lindén M, Rosenholm JB (2002) J Non-Crystal Solids 306:1
10. Sanchez C, Ribot F (1994) New J Chem 18:1007
11. Tian D, Dubois Ph, Jérôme R (1996) Polymer 37:3983
12. Tian D, Dubois Ph, Granfls Ch, Jérôme R, Viville P, Lazzaroni R, Brédas JL, Leprince P (1997) Chem Mater 9:871
13. Tian D, Dubois Ph, Jérôme R (1997) J Polym Sci Polym Chem 35:2295
14. Tian D, Blacher S, Dubois Ph, Jérôme R (1998) Polymer 39:855
15. Tian D, Blacher S, Pirard JP, Jérôme R (1998) Langmuir 14, 1905
16. Ahvenlammi J, Nousiainen P, Jokinen M, Peltola T (2000) In: Proceedings of the International Conference 'FiberMed 2000', Fibrous products in medical and health care. Fiber Technology and Clothing Science, Tampere University of Technology, Tampere, Finland, pp 175–185
17. Peltola T, Jokinen M, Veittola S, Rahiala H, Yli-Urpo A (2001) Biomaterials 22:589
18. Helminen A, Korhonen H, Seppälä JV (2001) Polymer 42:3345
19. Sarmento VHV, Dahmouche K, Santilli CV, Pulcinelli SH (2002) J Non-Crystal Solids 304:134
20. Watson H, Nordström A, Root A, Matisons J, Rosenholm JB (2001) J Adhesion Sci Technol 15:1103
21. Kursawe M, Glaubitt W, Blau C (1999) In: Vincenzini P (ed) Proceedings of the 9th Cimtec—World Forum on New Materials, Symposium, XI. Materials in clinical applications. Techna Srl, Florence, Italy, p 93
22. Brinker CJ, Assink RA (1989) J Non-Crystal Solids 111:48
23. Vallet-Regi M, Perez-Pariente J, Izquiredo-Barba I, Salinas A (2000) Chem Mater 12:3770
24. Areva S, Peltola T, Säilynoja E, Laajalehto K, Lindén M, Rosenholm JB (2002) Chem Mater 14:1614